Princeton Plasma Physics Laboratory

PPPL- 4699

PPPL- 4699

# X-ray Imaging Diagnostics For Magnetically Confined And Laser-produced Fusion Plasmas

N.A. Pablant, M. Bitter, L.F. Delgado-Apricio, K.W. Hill and M. Sanchez del Rio

October, 2011

Prepared for the U.S. Department of Energy under Contract DE-AC02-09CH11466.

# Princeton Plasma Physics Laboratory
# Report Disclaimers

---

## Full Legal Disclaimer

This report was prepared as an account of work sponsored by an agency of the United States Government. Neither the United States Government nor any agency thereof, nor any of their employees, nor any of their contractors, subcontractors or their employees, makes any warranty, express or implied, or assumes any legal liability or responsibility for the accuracy, completeness, or any third party's use or the results of such use of any information, apparatus, product, or process disclosed, or represents that its use would not infringe privately owned rights. Reference herein to any specific commercial product, process, or service by trade name, trademark, manufacturer, or otherwise, does not necessarily constitute or imply its endorsement, recommendation, or favoring by the United States Government or any agency thereof or its contractors or subcontractors. The views and opinions of authors expressed herein do not necessarily state or reflect those of the United States Government or any agency thereof.

## Trademark Disclaimer

Reference herein to any specific commercial product, process, or service by trade name, trademark, manufacturer, or otherwise, does not necessarily constitute or imply its endorsement, recommendation, or favoring by the United States Government or any agency thereof or its contractors or subcontractors.

---

# PPPL Report Availability

## Princeton Plasma Physics Laboratory:

http://www.pppl.gov/techreports.cfm

## Office of Scientific and Technical Information (OSTI):

http://www.osti.gov/bridge

---

**Related Links:**

**U.S. Department of Energy**

**Office of Scientific and Technical Information**

**Fusion Links**

# X-ray imaging diagnostics for magnetically confined and laser-produced fusion plasmas

N.A. Pablant[a], M. Bitter[a], L.F. Delgado-Aparicio[a], K.W. Hill[a], and M. Sanchez del Rio[b]

[a]Princeton Plasma Physics Laboratory, Princeton, New Jersey 08543, USA
[b]European Synchrotron Radiation Facility

August 22, 2011

## ABSTRACT

Recent advances in x-ray detection technology and diagnostic design have dramatically improved the ability of using x-ray imaging and spectroscopic diagnostics to accurately measure important parameters in magnetically confined and laser produced fusion plasmas. With these advancements, the detailed characterization of the diagnostic system properties has become ever more important. We present an overview of current and future x-ray diagnostic requirements for fusion plasmas and describe, in particular, diagnostic systems employing spherically bent crystals to resolving characteristic x-ray lines from trace impurities with energies in the range 1-20keV. The requirements and challenges for the simulation of existing and planned diagnostic installations and are discussed.

**Keywords:** Fusion, plasma, x-ray lines, curved crystal, imaging, spectroscopy

## 1. INTRODUCTION

The use of x-ray emission from magnetic confinement and laser-produced fusion research plasmas has been an essential non-perturbative diagnostic technique since the earliest experiments.[1, 2] Recent advances in x-ray diagnostic design[3–5] and detection technology[6], in particular the development of 2D pixel detectors, have dramatically improved the ability of x-ray imaging and spectroscopic diagnostics to accurately measure plasma parameters (temperature and rotation velocity). Here we present in particular the current status of diagnostics employing spherically bent crystals to study x-ray emission from trace impurities within the plasma. These include imaging x-ray crystal spectrometers[3, 4, 7, 8] which employ a single crystal in a 1D spectroscopic imaging configuration to measure profiles of the plasma ion and electron temperatures and plasma rotation velocities. This type of diagnostic is considered essential for providing temperature and rotation measurements on several existing fusion experiments and is planned to be installed on ITER, the next generation tokamak experiment. A second diagnostic instrument is presented for recording 2D images x-ray emission at a selected wavelength using matched pairs of spherically bent crystals.[5, 9, 10] Diagnostics utilizing both the 1D and 2D configurations have been proposed for use with laser-produced fusion plasmas at the National Ignition Facility (NIF).[11] These proposed diagnostics present unique design challenges due to the high spatial and temporal resolutions required.

### 1.1 Fusion research

There are two very different approaches to fusion energy currently being pursued: magnetic confinement fusion (MCF) and inertial confinement fusion (ICF). Both aim to generate energy though the fusing of deuterium and tritium into helium. The first approach, MCF, involves confining a plasma through the use of magnetic fields and is the basis of tokamak and stellarator devices. In these devices a plasma at relatively low densities ($n_e \approx 10^{20}\mathrm{m}^{-3}$) is brought to high temperatures ($T_e > 10\mathrm{keV}$) through the use of radio frequency or neutral particle heating. The goal of MCF is to create a steady state plasma discharge with constant heating and energy extraction. The flagship experiment aimed at achieving these goals is ITER, a new tokamak currently under construction in Cadarache, France though an international research collaboration.[12] In addition to being significantly larger than current devices ITER will operate at higher temperatures and

Advances in Computational Methods for X-Ray Optics II,
edited by Manuel Sanchez del Rio, Oleg Chubar, Proc. of SPIE Vol. 8141, 81410U

densities ($n_e \approx 10^{20}\text{m}^{-3}$ and $T_e \approx 30\text{keV}$). This presents a number of diagnostic challenges for which x-ray diagnostics are particularly well suited.[13]

The second approach to fusion, ICF, is through quick compression and heating of a small fuel pellet. Currently the most promising way to achieve this is though the use of powerful lasers. This results in very rapid discharges at high densities and temperatures ($n_e \approx 10^{32}\text{m}^{-3}$ and $T_e \approx 10\text{keV}$)[14]. For power generation a series of these quick discharges would be used at a rate of 10-20Hz.[15] The current state of the art experiment for ICF research is the National Ignition Facility (NIF) at the Lawrence Livermore National Laboratory.

## 1.2 X-ray diagnostics

Both MCF and ICF fusion approaches required a detailed understanding of the plasma dynamics, and therefore require advanced diagnostic capabilities. Given the high temperatures of fusion plasmas and the high energies released in the fusion reaction, emission from x-rays is a natural diagnostic tool to use. In addition, as fusion devices move toward reactor scales, many of the other diagnostics that are used on current devices will become ineffective or impractical, increasing the reliance on x-ray diagnostics.

X-ray based fusion diagnostics can be broadly divided into two types: those that rely on direct x-ray emission from the bulk plasma species and the fusion reaction, and those that rely on emission impurity species. For fusion diagnostic purposes, where high temperatures cause the bulk plasma species to become fully ionized, it is emission from highly charged high Z impurities that is of the most interest. This paper will focus on a specific set of x-ray diagnostics which view high energy x-rays from impurities by employing Bragg reflection from crystals as optical elements.

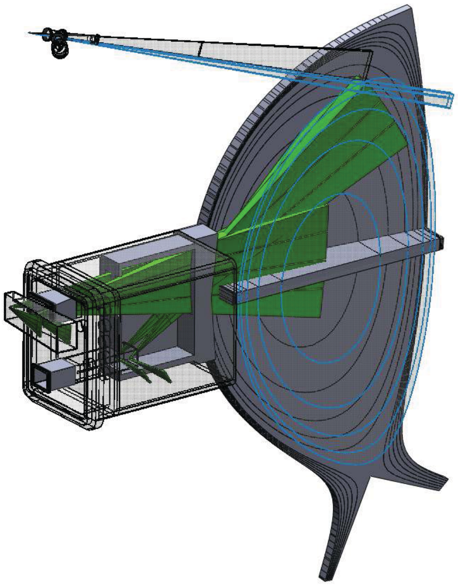

Figure 1: Proposed layout geometer for the ITER XICS system. Here both the core system (shown in green), which is a US undertaking, and the edge system, which is an Indian contribution, are shown. Both a radial view and a view with a tangential component are used to distinguish the toroidal($V_\phi$) and poloidal($V_\theta$) rotation velocities. In addition, to obtain coverage across the full minor radius, two arrays are needed, leading to a total of four XICS arrays for the core system. Image courtesy of R. Feder, PPPL.

# 2. HIGH RESOLUTION X-RAY IMAGING CRYSTAL SPECTROMETER FOR MAGNETIC CONFINEMENT FUSION EXPERIMENTS

There are a number of important plasma parameters that can be diagnosed through the use of x-ray emission from magnetically confined plasmas.[1] XICS diagnostics are able to measure time resolved profiles of the ion temperature ($T_i$), electron temperature ($T_e$) and plasma rotation ($V$). The rotation velocity profile is important in understanding and controlling the plasma stability, while measurements of the ion and electron temperature profile are important for plasma heating and the study of confinement modes and heat transport.

Recent developments in diagnostic design and detector technology have allowed tremendous advances in x-ray diagnostics in general, but particularly for the XICS diagnostic. This type of diagnostic in now installed at many of the major MCF fusion facilities including Alcator C-Mod[4, 16], NSTX[17], KSTAR[18] and EAST[19] and the Large Helical Device (LHD)[7, 8, 20], and is planed as the the primary core ion temperature and rotation velocity diagnostic for ITER[21][22]. This diagnostic technique is of particular importance for future devices, where other diagnostics, such as those based on charge exchange recombination spectroscopy (CER), are expected to encounter difficulties in making temperature and rotation measurements in the core due to poor penetration of the neutral beams that they rely on.[13] XICS based diagnostics have an additional advantage in that they are relatively simple to design and construct and can be adapted to many different plasma regimes.

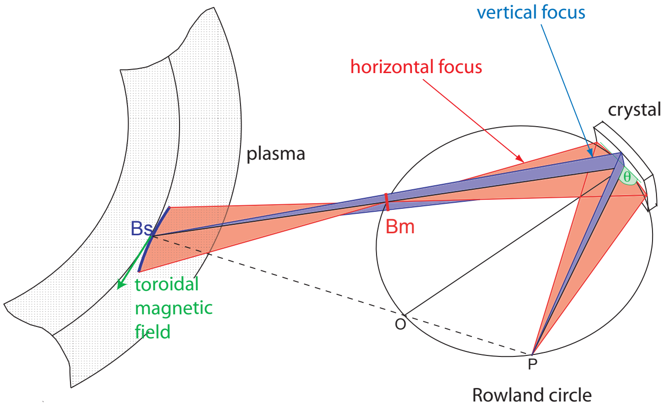

Figure 2: Conceptual diagram of the XICS diagnostic geometry. Shown is a representation of the light cone corresponding to a single pixel on the detector, point P, which is placed on the Rowland circle. Because of the astigmatism of a spherically bent reflector, one obtains two mutually perpendicular, meridional and sagittal, line foci of the point P at Bm and Bs, respectively. Imaging is done in the vertical direction, allowing a full vertical profile of the plasma to be recorded. Spectra are recorded in the horizontal direction on the camera based on the requirement that the Bragg condition is satisfied for the incoming x rays. Each wavelength corresponds to a range of toroidal angles due to the astigmatism (exaggerated in this diagram); this is the preferred experimental arrangement on tokamaks where the x-ray emissivity is uniform along the field lines. The arrangement shown has rotational symmetry about the line normal to the crystal center (which passes through the point O).

The XICS diagnostic utilizes a spherically bent crystal to provide a 1D image of line integrated spectra from highly charged impurity species in the plasma. A conceptual diagnostic layout is shown in Fig.2. Measurements of the plasma parameters are made by analyzing x-ray emission from highly charged, high Z impurities in the plasma. Measurements of the ion-temperature ($T_i$) are made from the Doppler broadening of the spectral lines, while the electron-temperature ($T_e$) can be found from the relative intensities of dielectronic satellite lines to resonant emission lines. With the appropriate viewing geometry, the Doppler shift of the lines can be used to measure the plasma rotation velocity. Local temperature and rotation values can be inferred from these line integrated spectra through tomographic inversion, which relies on a plasma equilibrium reconstruction. The XICS system can also play an important role for the monitoring of intrinsic impurities.

These impurity species that is used for these measurements can either be intrinsic to the experimental device, providing a truly non-perturbative measurement, or specifically introduced for diagnostic purposes. Noble gasses are generally preferred as injected impurities due to their low reactivity, however in principal any element can be used. At the temperatures routinely seen in current devices, $T$ =1–5keV, the typical impurities used are helium-like $Ar^{16+}$ and hydrogen-like $Ar^{17+}$. At the higher temperatures, such as those expected in ITER, helium-like Fe and neon-like W have been identified as favorable intrinsic impurities and helium-like Kr as an injected impurity. Other elements that have been previously used for x-ray crystal spectrometer (XCS) measurements are Ca[23], Ti[24], Cr [24], Fe[25][24] and Mo[26]. For plasma temperatures above 3keV, it is not generally possible to make measurements across the full plasma profile though the use of a single impurity species and charge state. In these cases the use of multiple systems, or multiple crystals within a single system are required for full coverage.

In order to produce hardware configurations for all of these various emission sources, a variety of crystal materials and lattice plains must be employed as the reflective element. Current systems use the following crystals with the given Miller indices: 110 quartz (LHD, KSTAR, EAST) or 102 Quartz (Alcator C-Mod), 422 germanium (NSTX) and 400 germanium (planned for ITER). To obtain a spherical shape, a thin crystal slice is placed onto a glass substrate and held in place though electrostatic forces. Typical sizes of the crystal that are used in these diagnostics are around 4cm × 10cm with a thickness of $150\mu$m.

The XICS diagnostic technique has benefited greatly by the development of x-ray detectors based on modern CMOS hybrid-pixel technology, in particular the Pilatus II detector developed by the Paul Scherrer Institute and is commercially produced by Dectris.[6][27] Each of these detectors comprises of ~100,000 pixels, and has a pixel pitch of $172\times172\mu\text{m}^2$. Each pixel has a high single-photon count rate capability of 2MHz and low neutron response. These detector modules are radiation hardened and have been tested to a fluence of $10^{14}$ 1MeV neutrons/$\text{cm}^{-2}$.

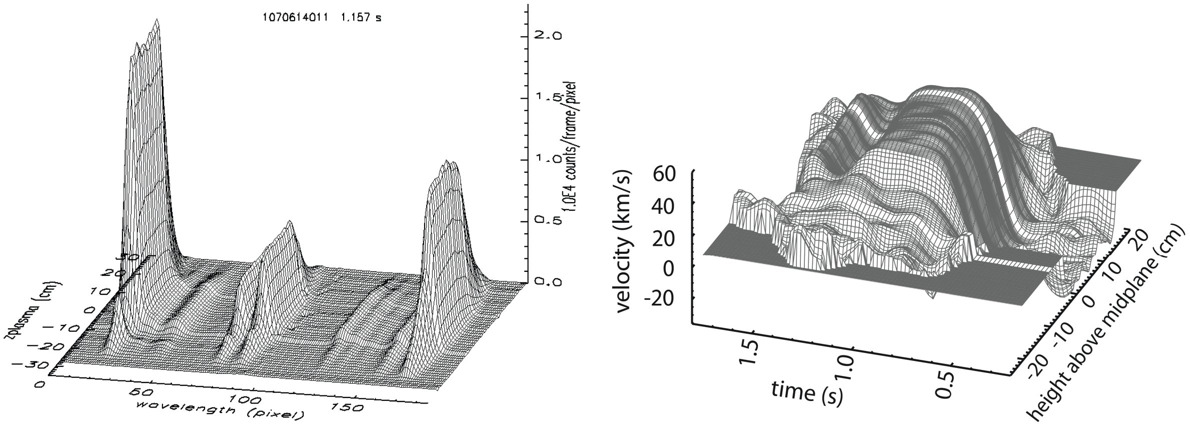

(a) Raw Spectra (b) Toroidal Velocity ($V_\phi$) (no inversion)

Figure 3: Data from the XICS system on Alcator C-Mod. (a) raw data for the spatially resolved spectral data for a single frame. (b) apparent velocity along the toroidal axis of the tokamak, obtained from the Doppler shifts of the emission lines.

## 2.1 Analysis techniques

The x-ray spectra recorded by the XICS diagnostic can be quite complicated due to multiple overlapping satellite lines (see Fig.3a). To accurately determine the intensity, width and location of the individual emission lines, spectral fitting using an atomic physics based spectral model is necessary. Currently the most accurate calculations for the line locations and for the relative intensities of the satellite lines can be obtained from the MZ code[28]. In order to compute the electron temperature, additional atomic physics is required, namely accurate excitation rate coefficients for both the resonance and satellite lines. Current analysis procedures use excitation rate coefficients calculated using the AUTOSTRUCTURE code.[29]

To accurately determine $T_i$ from the spectral fits it is necessary to separate the line broadening due to the Doppler effect from other line broadening effects. In these systems there are three primary sources of line broadening: Doppler broadening, natural line broadening and instrumental broadening. For a truly accurate fit the instrumental response must be characterized and convolved with the natural (Lorentzian) and Doppler (Gaussian) line shapes.

In order to find local values of the plasma parameters from the line integrated spectrum, an inversion of the data is required. This is possible with a reconstruction of the plasma equilibrium and a few assumptions: that the plasma emissivity and temperature are constant on flux surfaces and that the ion temperature distribution is Maxwellian. Typically this inversion process is done by approximating that a recorded spectrum can be treated as containing emission along a single line through the plasma. Analysis can be improved however by instead using the viewing volume associated with each detector element.

## 3. X-RAY DIAGNOSTICS FOR INTERNAL CONFINEMENT FUSION EXPERIMENTS

X ray diagnostics are one of the essential tools for ICF produced plasmas. There are several types of x-ray diagnostic schemes currently in use. These are either based on imaging x rays produced in the plasma or by using an external x ray source and measuring the absorption through the plasma.

For measuring emission from the plasma, there are a number of diagnostic possibilities that involve the use of crystal elements for x ray focusing. Two of these diagnostic possibilities have been recently been proposed for installation on the National Ignition Facility (NIF).[11]

### 3.1 X-Ray line shape diagnostic

It is possible to use a very similar diagnostic arrangement as described in Section 2 for x-ray line shape measurements from an ICF discharge. This type of diagnostic could potentially provide measurements of both the plasma temperature and density through fitting of the recorded x-ray spectra.[30] At the high densities achieved in ICF discharges, the effect on the x-ray line widths from Stark broadening will equal to or greater than that of Doppler broadening. To obtain a measurement of the temperature and density, these two effects must be distinguished, which requires high resolution spectroscopic measurements. In addition to line-shape measurements, it should also be possible to determine the electron temperature from line intensity ratios using this proposed diagnostic.

The configuration for this diagnostic is to place the plasma at the center of the sagittal focal line for the central wavelength. The location of the sagittal focus will vary over the wavelength range recorded, however if the diagnostic parameters are correctly chosen, the plasma will be within the focal line across the entire spectrum (see Ref. 11).

Similar to the XICS system, this configuration can in principle provide a 1D profile of the plasma. In this case though very high spatial resolution is required due to the small fusion targets. For NIF experiments the size of the plasma is approximately $100\mu$m. Simple estimations indicate that a resolution of $\approx 5\mu$m may be possible, however detailed ray tracing of potential diagnostic layouts, with realistic values for the crystal diffraction profile, will be necessary to realistically evaluate the feasibility of spatially resolved measurements. however, even as a spatially averaged measurement this diagnostic could be very valuable diagnostic addition to the NIF experimental program.

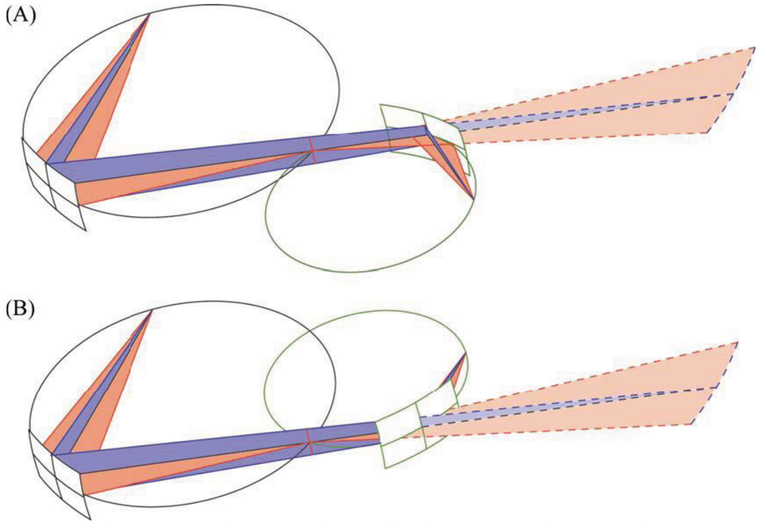

Figure 4: Stigmatic imaging schemes employing spherically bent crystals. To achieve point to point imaging the radii of curvature and angles of incidence (or Bragg angles) are chosen so that the sagittal and meridional foci from each crystal are coincident. In diagrams above the sagittal focus is real for one crystal and virtual for the other. Arrangements are also possible where the sagittal focus is real for both crystals. For imaging of x rays the Bragg condition must also be matched. This requires the additional constraint that the primary spherical aberration, known as the Johann error[31], is also matched between the two crystals.

## 3.2 Stigmatic imaging X-ray diagnostics

By using two matched spherical crystals it is possible to devise a stigmatic imaging scheme for x rays. The details of the matching conditions needed for this type of scheme has been described by Bitter *et al.* in Ref. 5. This type of imaging arrangement provides a nearly monochromatic image of the plasma, the wavelength of which is determined by the choice of crystals and Bragg angles. This scheme has an advantage over a simple pinhole camera in that the crystals and detector can be placed further from the ICF target while still providing a much greater photon throughput.[11]

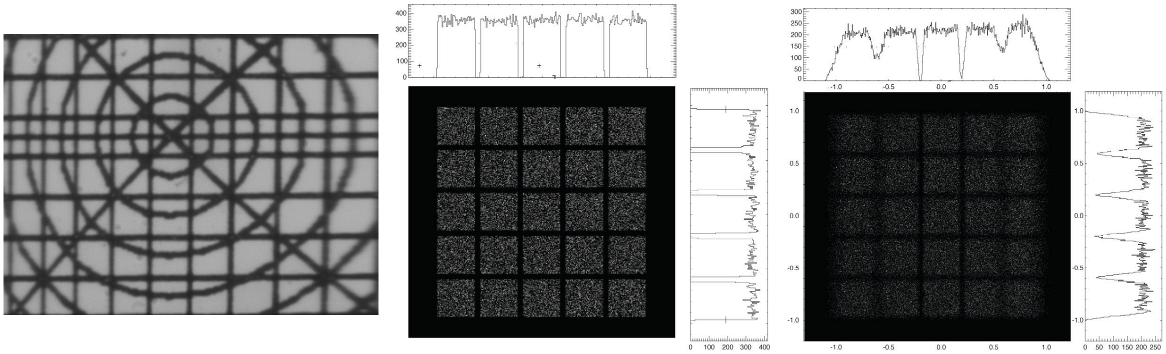

(a) Raw Spectra (b) Source pattern (c) Image of the source pattern.

Figure 5: Ray tracing and experimental results using in visible light using the imaging scheme shown in Fig.4b. (a) Experimental results in visible light using a printed with a line thickness of 50$\mu$m. 50mm diameter lenses were used. Features smaller than 50$\mu$m can clearly be seen. (b & c) Results from preliminary ray tracing simulations were performed using the SHADOW code[32]. (b) A flat emitter of $2 \times 2mm^2$ patterned with a mesh (40$\mu$m period, 50$\mu$m thick), was placed at the focal point. The source fully illuminates the first mirror of 50 mm diameter. (c) The optical image at the detector location demonstrates that the patterned source is fully resolved, with slightly better resolution in the sagittal direction. The imaging fidelity is better in the central portion of the figure, in agreement with the observed experimental image.

Experimental verification of these imaging schemes have been done using visible light with promising results (see Fig.5a). Ray tracing simulations for the visible light case have also been completed using the `SHADOW`[32] code showing agreement with experiment, as can be seen in Fig.5b & 5c. Efforts to better characterize this diagnostic scheme are continuing and experiments to explore the performance of these schemes using x rays are currently underway at Princeton Plasma Physics Laboratory (PPPL) along with continuing efforts at the European Synchrotron Radiation Facility (ESRF) to incorporate the effect of the crystal diffraction profile on the imaging performance.

## 4. SIMULATION OPPORTUNITIES FOR X-RAY IMAGING AND SPECTROSCOPIC DIAGNOSTICS

In the past the measurement accuracy achievable by XICS diagnostics was primarily limited by the detector technology and the accuracy of atomic physics calculations. Recent advances in detector technology, diagnostic design, analysis techniques and atomic physics codes have dramatically improved these diagnostics systems. Accurate system characterization, spectral analysis and tomographic inversion are increasingly important for further improvements to the diagnostic performance. Computer simulation may now play a determinant role in the design and optimization of these systems, and can play an important role in calibration procedures. This is of particular interest for diagnostic systems on the next generation of fusion devices, such as ITER, which need to obtain high quality measurement with much more severe design constraints. The ability to fully model potential optical configurations using ray tracing is important for optimization of these systems. In addition, new fast and performant data analysis applications will be necessary to perform spectral analysis and tomographic inversion of a high amount of experimental data.

A number of topics have been identified where computer modeling of optical systems combined with data analysis and data prediction can play an important role in future development of these diagnostics:

- **Accurate determination of the instrumental response of the system.** In order to accurately fit the recorded spectrum, it is necessary to know how emission from the plasma at a specific wavelength will be distributed on the detector. This includes the effects of optical aberrations from the crystal element, the effect of the width of the crystal diffraction profile, and geometrical effects such as the crystal dimensions and detector position. While the instrumental response can be approximated fairly accurately through either analytical calculations[33] or simple ray-tracing, there are subtleties that require a more detailed analysis to quantify, such as the effects of polarization of the plasma emission. The use of multiple optical elements, such as the two crystal imaging system described here, makes analytical calculations cumbersome and the use of powerful simulation tools becomes a necessity. An example of some preliminary simulations of the XICS configuration is shown in Fig.6.

  Characterization of the instrumental response must also be extended to include emission from any calibration sources. For accurate measurement of absolute plasma flow velocities, an extremely accurate wavelength calibration is needed. The most promising method for achieving this is through the *in-situ* use of an x-ray florescence source. Modeling of the emission and expected response from such a source on the detector will improve the accuracy of this kind of calibration technique.

- **Variations of the crystal temperature.** Changes to the crystal temperature will affect the crystal spacing and therefore the properties of the Bragg reflection. Even small temperature changes to the crystal temperature, on the order of 1°C, can lead to significant errors in the measured plasma properties, especially the plasma rotation velocity.[34] Heating of the crystal is possible both through the energy incident on the crystal from plasma emission and through the surrounding environment. Active cooling may used to stabilize the crystal temperature, but complications, such rapid heating due to incident radiation from transient plasma events, should be taken into consideration. Finite Element Calculations (FEM) could be used to help in the study of thermal deformations and to optimize a cooling system. A dedicated system to predict the crystal d-spacing based on a measured surface temperature history, including any hysteresis effects, may be essential for accurate data analysis.

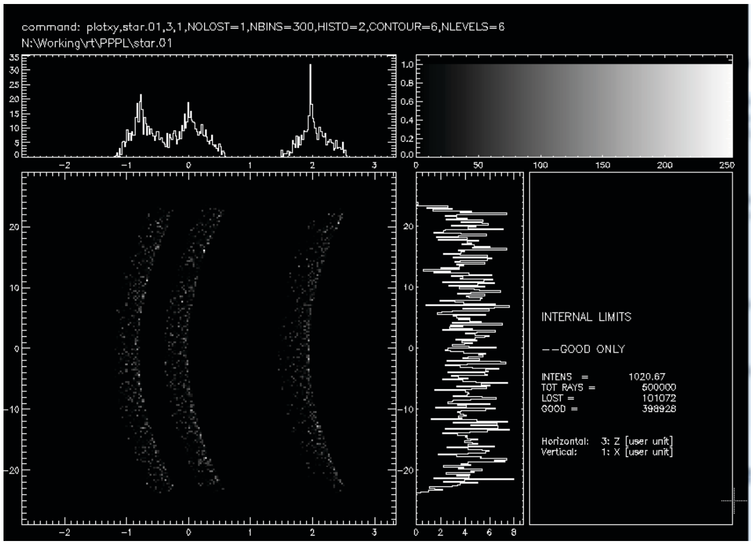

```
command: plotxy,star.01,3,1,NOLOST=1,NBINS=300,HISTO=2,CONTOUR=6,NLEVELS=6
N:\Working\rt\PPPL\star.01
```

```
INTERNAL LIMITS

--GOOD ONLY

INTENS  =         1020.67
TOT RAYS =         500000
LOST =             101072
GOOD =             398928

Horizontal:   3: Z [user unit]
Vertical:     1: X [user unit]
```

Figure 6: Ray tracing simulation of the XICS configuration shown in Fig.2 using the `SHADOW` code[32]. Shown is the image produced on the detector plane produced by a point source with three lines, at wavelengths of 3.9494$\mathring{A}$, 3.9624$\mathring{A}$ and 3.9944$\mathring{A}$. The source is placed 329mm from a 101 quartz-like crystal, with radius 555mm. Note the different horizontal and vertical scales. Units are mm.

- **Radiation damage by neutron and gamma fluence on the crystal.** In future reactors the crystal will be subject to a large flux of high energy particles. High energy neutrons will be produced by the fusion reaction ($^2_1D + ^3_2T \rightarrow ^4_2He$ (3.5MeV) $+ n$ (14.1MeV)), and these will in turn also produce additional neutron and gamma radiation through interactions with the surrounding materials. This high energy radiation may irreversibly degrade the structure of the crystal, affecting the reflectivity and diffraction profile, and thus introducing a mosaicity. It is very difficult to perform experiments to characterize this neutron damage since neutron sources with similar energy spectra and fluence do not exist. While it may be possible to use in-situ calibration techniques to determine the extent of the crystal damage, predictive capability is needed before the installation of such a diagnostic to determine the expected diagnostic lifetime. For that purposes Monte Carlo simulations of the neutron interaction with the crystal material, and the release and transport of secondary particles may be used to estimate the energy deposition in the crystal and therefore infer the type of degradation that could be expected.

So far the diagnostics systems described have used spherically bent mirrors. Spherical mirrors have been chosen both for their simplicity and for their ease of manufacturing. Another area that needs further investigation is the use of optimized aspheric shapes for the improvement of diagnostic performance. The use of aspheric elements may be of particular importance for 2D stigmatic imaging schemes presented.

## ACKNOWLEDGMENTS

Research supported by the U.S. DOE under Contract No. DE-AC02-09CH11466 with Princeton University.

## REFERENCES

[1] Stratton, B. C., Bitter, M., Hill, K. W., Hillis, D. L., and Hogan, J. T., "Passive spectroscopic diagnostics for magnetically confined fusion plasmas," *FUSION SCIENCE AND TECHNOLOGY* **53**, 431–486 (FEB 2008).

[2] Bitter, M., Hsuan, H., Hill, K. W., and Zarnstorff, M., "X-ray diagnostics of tokamak plasmas," *Physica Scripta* **T47**, 87–95 (1993).

[3] Bitter, M., Hill, K. W., Stratton, B., Roquemore, A. L., Mastrovito, D., Lee, S. G., Bak, J. G., Moon, M. K., Nam, U. W., Smith, G., Rice, J. E., Beiersdorfer, P., and Fraenkel, B. S., "Spatially resolved spectra from a new x-ray imaging crystal spectrometer for measurements of ion and electron temperature profiles (invited)," *Review of Scientific Instruments* **75**(10), 3660–3665 (2004).

[4] Ince-Cushman, A., *Rotation Studies in Fusion Plasmas via Imaging X-ray Crystal Spectroscopy*, PhD thesis, Massachusetts Institute of Technology (September 2008).

[5] Bitter, M., Delgado-Aparicio, L., Hill, K. W., Scott, S., Ince-Cushman, A., Reinke, M., Podpaly, Y., Rice, J. E., Beiersdorfer, P., and Wang, E., "Imaging with spherically bent crystals or reflectors," *Journal of Physics B: Atomic, Molecular and Optical Physics* **43**(14), 144011 (2010).

[6] Broennimann, C., Eikenberry, E., Henrich, B., Horisberger, R., Huelsen, G., Pohl, E., Schmitt, B., Schulze-Briese, C., Suzuki, M., Tomizaki, T., et al., "The PILATUS 1M detector," *J. Synchrotron Rad.* **13**(2), 120–130 (2006).

[7] Bitter, M., Hill, K., Gates, D., Monticello, D., Neilson, H., Reiman, A., Roquemore, A. L., Morita, S., Goto, M., Yamada, H., and Rice, J. E., "Objectives and layout of a high-resolution x-ray imaging crystal spectrometer for the large helical device," *Review of Scientific Instruments* **81**(10), 10E328 (2010).

[8] Pablant, N. A., Bitter, M., Delgado-Aparicio, L., Goto, M., Hill, K., Lazerson, S., Morita, S., Roquemore, A., Gates, D., Monticello, D., Nielson, H., Reiman, A., Reinke, M., Rice, J., and Yamada, H., "First results from the high-resolution x-ray imaging crystal spectrometer on the large helical device," to be submitted to RSI (2011).

[9] Bitter, M., Hill, K. W., Scott, S., Feder, R., Ko, J., Ince-Cushman, A., and Rice, J. E., "Wide-angle point-to-point x-ray imaging with almost arbitrarily large angles of incidence," *Review of Scientific Instruments* **79**(10), 10E927 (2008).

[10] Bitter, M., Hill, K. W., Jones, F., and Scott, S., "Non-astigmatic imaging with matched pairs of spherically bent crystals or reflectors.," *Journal of X-Ray Science & Technology* **17**(2), 153 – 160 (2009).

[11] Bitter, M., Hill, K., Pablant, N., Delgado-Aparicio, L., Beiersdorfer, P., Wang, E., and Sanchez del Rio, M., "X-ray line-shape diagnostics and novel stigmatic imaging schemes for the national ignition facility," in [*Proceedings of the 38th EPS Conference on Plasma Physics*], (2011).

[12] Shimada, M. et al., "Progress in the iter physics basis - chapter 1: Overview and summary," *Nuclear Fusion* **47**(6), S1 (2007).

[13] Donné, A. et al., "Progress in the iter physics basis - chapter 7: Diagnostics," *Nuclear Fusion* **47**(6), S337 (2007).

[14] Glenzer, S. H. et al., "Demonstration of ignition radiation temperatures in indirect-drive inertial confinement fusion hohlraums," *Phys. Rev. Lett.* **106**, 085004 (Feb 2011).

[15] Moses, E. I., "The national ignition facility and the promise of inertial fusion energy," *FUSION SCIENCE AND TECHNOLOGY* **60**, 11–16 (JUL 2011). 19th Topical Meeting on the Technology of Fusion Energy (TOFE-19), Las Vegas, NV, NOV 08-11, 2011.

[16] Hill, K. W., Bitter, M. L., Scott, S. D., Ince-Cushman, A., Reinke, M., Rice, J. E., Beiersdorfer, P., Gu, M.-F., Lee, S. G., Broennimann, C., and Eikenberry, E. F., "A spatially resolving x-ray crystal spectrometer for measurement of ion-temperature and rotation-velocity profiles on the alcator c-mod tokamak," *Review of Scientific Instruments* **79**(10), 10E320 (2008).

[17] Bitter, M., Hill, K., Roquemore, L., Beiersdorfer, P., Thorn, D., and Gu, M. F., "Results from the national spherical torus experiment x-ray crystal spectrometer," *Review of Scientific Instruments* **74**(3), 1977–1981 (2003).

[18] Lee, S. G., Bak, J. G., Nam, U. W., Moon, M. K., Shi, Y., Bitter, M., and Hill, K., "The first experimental results from x-ray imaging crystal spectrometer for kstar," *Review of Scientific Instruments* **81**(10), 10E506 (2010).

[19] Shi, Y., Wang, F., Wan, B., Bitter, M., Lee, S., Bak, J., Hill, K., Fu, J., Li, Y., Zhang, W., Ti, A., and Ling, B., "Imaging x-ray crystal spectrometer on east," *Plasma Physics and Controlled Fusion* **52**(8), 085014 (2010).

[20] Pablant, N. A., Bitter, M., Delgado-Aparicio, L., Goto, M., Hill, K., Lazerson, S., Morita, S., Roquemore, A., Gates, D., Monticello, D., Nielson, H., Reiman, A., Reinke, M., Rice, J., and Yamada, H., "Layout and expected performance of the recently installed high-resolution x-ray imaging crystal spectrometer on the large helical device," in [*Proceedings of the 38th EPS Conference on Plasma Physics*], (2011).

[21] Beiersdorfer, P., Clementson, J., Dunn, J., Gu, M. F., Morris, K., Podpaly, Y., Wang, E., Bitter, M., Feder, R., Hill, K. W., Johnson, D., and Barnsley, R., "The iter core imaging x-ray spectrometer," *Journal of Physics B: Atomic, Molecular and Optical Physics* **43**(14), 144008 (2010).

[22] Hill, K. W., Bitter, M., Delgado-Aparicio, L., Johnson, D., Feder, R., Beiersdorfer, P., Dunn, J., Morris, K., Wang, E., Reinke, M., Podpaly, Y., Rice, J. E., Barnsley, R., O'Mullane, M., and Lee, S. G., "Development of a spatially resolving x-ray crystal spectrometer for measurement of ion-temperature (t[sub i]) and rotation-velocity (v) profiles in iter," *Review of Scientific Instruments* **81**(10), 10E322 (2010).

[23] Howard, N. T., Greenwald, M., and Rice, J. E., "Characterization of impurity confinement on alcator c-mod using a multi-pulse laser blow-off system," *Review of Scientific Instruments* **82**(3), 033512 (2011).

[24] Morita, S. and Goto, M., "X-ray crystal spectrometer with a charge-coupled-device detector for ion temperature measurements in the large helical device," *Review of Scientific Instruments* **74**(4), 2375–2387 (2003).

[25] Bitter, M., Hill, K. W., Sauthoff, N. R., Efthimion, P. C., Meservey, E., Roney, W., von Goeler, S., Horton, R., Goldman, M., and Stodiek, W., "Dielectronic satellite spectrum of heliumlike iron (fe xxv)," *Phys. Rev. Lett.* **43**, 129–132 (Jul 1979).

[26] Delgado-Aparicio, L., "Formation, stability and momentum transport characteristics of impurity-induced snakes in alcator c-mod," in [*Proceedings of the 38th EPS Conference on Plasma Physics*], (2011).

[27] "http://www.dectris.com/sites/pilatus100k.html," (03 2010).

[28] Goryayev, F., Urnov, A., and Vainshtein, L., "Atomic data calculations by z-expansion method for doubly excited states 2lnl'and 1s2lnl'of highly charged ions with z= 6-36. i. transitions from the states with n= 2, 3," *Arxiv preprint physics/0603164* (2006).

[29] Marchuk, O., *Modeling of He-like spectra measured at the tokamaks TEXTOR and TORE SUPRA*, PhD thesis, Ruhr-Universität Bochum (2004).

[30] Florido, R., Mancini, R., Nagayama, T., Tommasini, R., Delettrez, J., Regan, S., Smalyuk, V., Rodríguez, R., and Gil, J., "Argon k-shell and bound-free emission from omega direct-drive implosion cores," *High Energy Density Physics* **6**(1), 70 – 75 (2010).

[31] Johann, H. H., "Die erzeugung lichtstarker röntgenspektren mit hilfe von konkavkristallen," *Zeitschrift für Physik A Hadrons and Nuclei* **69**, 185–206 (1931). 10.1007/BF01798121.

[32] Cerrina, F. and Sanchez del Rio, M., [*Handbook of Optics, Volume V: Atmospheric Optics, Modulators, Fiber Optics, X-Ray and Neutron Optics*], vol. 5, ch. 35: Ray Tracing of X-Ray Optical Systems, McGraw-Hill Professional (2009).

The Princeton Plasma Physics Laboratory is operated
by Princeton University under contract
with the U.S. Department of Energy.

Information Services
Princeton Plasma Physics Laboratory
P.O. Box 451
Princeton, NJ 08543

Phone: 609-243-2245
Fax: 609-243-2751
e-mail: pppl_info@pppl.gov
Internet Address: http://www.pppl.gov